

# Training point-based deep learning networks for forest segmentation with synthetic data

Francisco Raverta Capua<sup>1</sup>[0009-0004-3337-7741], Juan Schandin<sup>2</sup>[0009-0009-9994-3503], and Pablo De Cristóforis<sup>1,2</sup>[0000-0002-7551-7720]

<sup>1</sup> Instituto en Ciencias de la Computación (UBA-CONICET), Ciudad Autónoma de Buenos Aires C1428EGA, Argentina

`fraverta@icc.fcen.uba.ar`

<sup>2</sup> Departamento de Computación, Facultad de Ciencias Exactas y Naturales, Universidad de Buenos Aires, Ciudad Autónoma de Buenos Aires C1428EGA, Argentina

`{jschandin,pdecris}@dc.uba.ar`

**Abstract.** Remote sensing through unmanned aerial systems (UAS) has been increasing in forestry in recent years, along with using machine learning for data processing. Deep learning architectures, extensively applied in natural language and image processing, have recently been extended to the point cloud domain. However, the availability of point cloud datasets for training and testing remains limited. Creating forested environment point cloud datasets is expensive, requires high-precision sensors, and is time-consuming as manual point classification is required. Moreover, forest areas could be inaccessible or dangerous for humans, further complicating data collection. Then, a question arises whether it is possible to use synthetic data to train deep learning networks without the need to rely on large volumes of real forest data. To answer this question, we developed a realistic simulator that procedurally generates synthetic forest scenes. Thanks to this, we have conducted a comparative study of different state-of-the-art point-based deep learning networks for forest segmentation. Using created datasets, we determined the feasibility of using synthetic data to train deep learning networks to classify point clouds from real forest datasets. Both the simulator and the datasets are released as part of this work.

**Keywords:** Deep Learning · Point Cloud Segmentation · Forest Simulator

## 1 Introduction

The use of remote sensing for environmental monitoring has grown significantly in recent years, thanks to the development of Terrestrial Laser Scanning (TLS), Aerial Laser Scanning (ALS), and Aerial Photogrammetry, techniques widely used in precision forestry [1]. Both LiDAR and camera sensors made it possible to easily acquire three-dimensional data of the studied environment, accurately representing it with high precision level point clouds. Both have been widely used

in forest environments for health monitoring, species classification, tree parameter estimation, and even illegal logging detection amidst other applications [2]. Laser scanning, while more expensive, heavier, and energy-consuming, is considered the most accurate method for estimating the forest structure, as both the canopy and the ground can be detected [3].

Deep learning architectures, popular in natural language and image processing nowadays, have recently been extended to point cloud processing, and multiple techniques have already been adapted to the goals of classification, segmentation, and point completion [4].

Unfortunately, few point cloud datasets are publicly available for training, validating, and testing deep learning architectures, among which we can mention ScanNet [5], ScanObjectNN [6] and ModelNet40 [7] for object classification and ShapeNetPart [8] and SemanticKITTI [9] for part segmentation and scene completion. Generally speaking, none of them are designed for specific environments, such as forests. Therefore, if training a deep learning architecture for forested environment is needed, a new dataset for this purpose has to be generated. For example, [10] developed a dataset from the regions of the Southern Sierra Nevada Mountains, USA, [11] from Australia and New Zealand, and [12] from Evo, Finland. All these works were conducted for forest segmentation. Of the three, only the latter dataset is publicly available, limiting the repeatability of the experiments and the comparison between the cited works.

Creating a specific point cloud dataset for forested environments is expensive, as high-end equipment, including UAVs and high-precision sensors, is required to survey the studied area. It is also time-consuming, as it implies labeling the points manually. Moreover, forest areas could be inaccessible or dangerous for humans, further complicating data collection.

This work aims to answer whether synthetic data for training point-based deep learning networks is suitable for segmenting real forest point clouds generated from LiDAR or camera sensors. For this purpose, we developed a forest simulator based on Unity [13] that allows us to generate several forested scenes with high realism procedurally. We extract the point clouds from the synthetic scenes, which are then used to train the deep learning architectures instead of using real forest data. The main contributions of this work are as follows:

1. The development of a novel open-source forest simulator based on Unity that procedurally generates forest scenes. It also includes a configurable survey mission planner mode that takes pictures of the scene like a camera from an up-down UAV view.
2. Public-domain synthetic datasets of forest scenes that can be used to train or test different deep-learning networks.
3. A comparative study of state-of-the-art point-based deep learning networks to determine whether training with synthetic data is suitable for segmenting point clouds from real forest datasets.

This paper is organized as follows: Section 2 overviews related works. Section 3 briefly explains the deep-learning architectures selected for this work, and presents the developed forest simulator and the dataset generation. Section 4

shows and discusses the experimental results, and Section 5 ends with conclusions and future work.

## 2 Related Work

The development of TLS, ALS and aerial photogrammetry, aided with computer vision techniques, has made acquiring an accurate 3D reconstruction of the studied environment possible. This allows us to extract valuable information for the characterization, monitoring, and conservation of forests.

Thanks to the ability of the deep learning networks to adapt to several tasks, such as classification, segmentation, and completion, its use has expanded to several applications, including the study of different natural environments. For example, [14,15] use deep learning techniques for the extraction of digital terrain models (DTM) from camera images and [16] uses them for landform classification. Specifically in point cloud processing, [10,17,18,19] use deep learning for the extraction of DTM from LiDAR captured data. In a forest environment, [11] segments the LiDAR captured point cloud into different categories: terrain, vegetation, coarse woody debris (CWD) and stems. It is noticeable that segmenting the terrain from the rest of the points results equivalent to finding the DTM of the studied environment. Similarly, [12] uses segmentation techniques to classify the points into terrain, understorey, tree trunk, or foliage categories; the labeled point cloud dataset used in this work is one of the few publicly available.

The development of deep learning architectures designed for point cloud processing started to receive more attention with PointNet++ [20]. This architecture was taken as a starting point and as a comparison model for several new networks that seek to classify or segment point clouds. PointNet++ is based on a U-Net architecture [21] built mostly with multi-layer perceptrons with an encoder-decoder structure, where the encoder extracts features from point clouds, and the decoder reinterprets the extracted features. Several networks have been based on PointNet++, such as KPConv [22], PointConv [23], ConvPoint [24], which incorporated their own convolutional operator designed to work with point clouds, and PFCN [25], which was implemented using a fully convolutional network. PointNeXt [26] updates PointNet++ to the state-of-the-art using more modern training strategies, such as newer optimization techniques, data augmentation, and modifications of the architecture.

Transformer technology, based entirely on self-attention layers [27], presents advantages over the more standardized use of convolutional layers and multi-layer perceptrons in encoder-decoder architectures. This translates into more accurate results with lower training time as they are more parallelizable but at the cost of using a greater number of parameters, which requires a greater volume of input data for training. The first networks that incorporated transformer technology for point cloud processing were Engel’s PointTransformer [28], Zhao’s PointTransformer [29], Fast Point Transformer [30] and PCT [31], all of which try to adapt the structure of transformers into the point cloud data type. Following the same idea, PointBERT [32], that follows the ideas of BERT [33] and BEiT [34]

for natural language processing and image processing respectively, divides the point cloud into several smaller local clouds, and codifies each of them into tokens through a Discrete Variational AutoEncoder [35]. It then masks a given proportion of the local clouds and uses them as an input to the transformer block built with attention encoders only, which is trained to recover the original tokens of the masked clouds. Then it recovers the clouds from the tokens via a Decoder, and reconstructs the full point cloud.

Along the same lines, PointMAE [36] follows the ideas of MAE [37] for Image Processing, dividing the point cloud into smaller local clouds which are masked without the need for a Discrete Variational AutoEncoder. PointGPT [38], inspired by GPT [39], also divides the point cloud into smaller local clouds but orders them using a Morton curve by spatial proximity [40]. It then masks a given proportion of the local clouds with a dual mask strategy and uses them as an input to the transformer block built exclusively with attention decoders. It aims to predict future representations of local clouds in an autoregressive way.

Regarding the use of synthetic datasets in forest environments, in [41], a simulator is presented using procedural techniques, where sensors like LiDAR, an RGB camera, and a depth camera are also simulated for data extraction, all of them with the capacity of segmenting the scene in the following categories: background, terrain, traversable, trunks, canopy, shrubs, herbaceous plants, and rocks. A synthetic dataset using this simulator is available in [42]. It includes RGB images, semantic segmentation maps, depth maps and the projection of LiDAR point clouds on the RGB field of view for two different LiDAR scanning patterns. However, this simulator is not publicly available, and the dataset does not include the 3D reconstruction neither the point clouds dataset of the environment. Finally, [43] uses this dataset’s images for training networks to detect fuel for preventing spread of forest fires. This work concludes that the synthetic data fails to generalize to real data.

### 3 Materials and Methods

#### 3.1 Point cloud deep learning networks

Following [12], we aim to train different deep learning networks to segment the forest point clouds into trunks, canopy, understorey, and terrain. This lets us differentiate forest strata and the DTM that corresponds with the terrain points. We selected four well-known state-of-the-art architectures, PointNeXt, PointBERT, PointMAP, and PointGPT, and trained them with synthetic data generated by our forest simulator. Of these four selected architectures, the last three are built using transformers, and pre-trained versions are available with the ShapeNetPart dataset, so these networks can be fine-tuned specializing them in the respective study area. On the other hand, PointNext is not built using transformers but multi-layer perceptrons, and as we do not count on pre-trained versions of the network, we train it from scratch.

### 3.2 Forest Simulator

For this work, a forest simulator based on the Unity engine was developed, from which synthetic data with a similar appearance to real-world forests was extracted. We aim to train the mentioned architectures with synthetic data and test their performance with real forest data. As [12] notices, the manual labeling of the extracted point cloud is a very demanding task, and in several cases, it is impossible to human experts to discern which category each point belongs to. Using a simulator for dataset generation overcomes this problem, as the point cloud labeling can be carried out automatically. Moreover, as transformer technology requires a large volume of data for training, generating synthetic data procedurally becomes even more relevant. Below we detail the most important modules of the presented simulator.

**Terrain generation** The simulator first generates a terrain mesh using fractal noise to build a heightmap for all its vertices. These noise samples are from Perlin noise layers at different scales or octaves. This permits controlling the amount of detail and the general aspect of the terrain. As the implementation is easily parallelizable, we took advantage of the Perlin noise function provided by Unity and the Unity Jobs framework for parallel execution. The random appearance and realistic aspect of this method’s results are notorious and well-regarded in the video game developers community.

**Trees, bushes, and plants generation** Vegetation (excluding grass) is generated via pipelines. Each pipeline is a Directed Acyclic Graph (DAG) that links prefabs (i.e. reusable pre-generated game objects, like individual trees or bushes) with their position over the terrain. This is done through textures that determine the spawn probability and density over the terrain mesh. Each pipeline is built using different nodes:

- Source: imports a texture from a file or another pipeline, or generates a new one via a Voronoi diagram or sampling noise.
- Logic: applies logic operations over textures
- Sampling: variants of Poisson disk sampling method.
- Placement: generates instancing parameters for the assigned prefabs.

Regarding the sampling process, an implementation of Bridson’s Poisson disk sampling method [44] and a variation of it were implemented. In Bridson’s original algorithm, given an object  $a_0$  with radius  $r$ , new objects of the same radius are added in an annulus of size  $[r, 2r]$  without overlapping, until it reaches a maximum quantity, or until there can not be placed any more, and then this process is repeated with the next object. Using a cell size of  $r/\sqrt{n}$ , where  $n$  is the dimension of the background grid for storing samples, each cell can contain only one placed object. This process is fast for object placement, but it produces a distribution of points that may appear equidistant, especially for small values



Fig. 1: Sample models of trees used in the simulator, generated with software TreeIt [45].

of  $r$  giving an unrealistic point distribution. To face this issue we propose a variation to the method: new points are seeked in an annulus of size  $[r_{min}, r_{max}]$ , where  $r_{min}$  and  $r_{max}$  are a given minimum radius and a maximum radius respectively, interpolating the distance linearly using the value of a greyscale texture at each point. This means that for values near 0 (where the texture is black), points at a distance  $r_{min}$  from  $a_0$  are generated, and the inverse holds for values near 1. To do that, we tweaked Bridson’s algorithm to use a spatial cell of size  $r_{min}/\sqrt{n}$ , but instead of each cell holding the index of only one placed object, it holds a list of indices for the objects that shadow that cell and remains at an acceptable distance between themselves.

The texture of spawn probability acts as the probability of effectively instantiating an object at a given point. Having this as a separate node from the sampling process is useful since the number of objects spawned in an area can effectively be reduced, even to 0, making clearings of arbitrary shapes possible.

There can be created as many pipelines as required. The simulator already counts with basic pipelines for trees and bushes. The prefab models of trees, bushes, and other plants were generated with the free-to-use TreeIt software [45]. A small sample of them can be seen in Fig. 1. More models can be easily added if needed. Before instantiating these models, some transformations are applied to include more variability to the scene: a random spin around its up axis, a random twist to bend the up direction with regards to the world’s up direction, and a random scale.

**Grass generation** None of the sampling methods for vegetation distribution could scale to generate millions of points while keeping the frame rate manageable. Thus, a parallelizable method was devised for placing grass. It is generated by indirect instancing, where the geometry is produced via a compute shader (a program that run on the GPU, outside of the normal rendering pipeline) and sent to the graphics pipeline through a shared memory buffer. The sampling algorithm for the grass leaves is depicted in Algorithm 1. As the tiles are non-overlapping, the processing for each tile can be parallelized over the number of tiles. The generated points are then transformed into the terrain coordinates using parallel raycasting. For a  $256 \times 256$  pixels texture, a tile size of 4 pixels

**Algorithm 1** Grass Sampling

---

**Input:** texture  $T$ , tile size  $t_s$ , maximum number of points for a tile  $P$   
**Output:** points for grass leaf instancing  $G$

- 1: Divide the texture  $T$  into non-overlapping tiles according to a tile size  $t_s$
- 2: Define an empty list  $G$  for the points for grass instancing
- 3: **for** each tile  $t$  **do**
- 4:     Define density  $d = \frac{1}{t_s^2} \sum_{(i,j) \in t} p_{i,j}$ , where  $p_{i,j}$  is the texture’s value in pixel  $(i, j)$
- 5:     Define the number of sampling points in  $t$  by  $p = d \times P$
- 6:     Define points  $G_t$  by distributing  $p$  in a grid-like pattern in the tile
- 7:     Append  $G_t$  to  $G$
- 8: **end for**
- 9: **return** generated points  $G$

---

and a maximum of 1024 points per tile, the shader takes less than one second to run approximately 4 million points, running in an Intel Core i9-10900 processor, with 32 GB RAM and a NVIDIA GTX 1060 board.

The points are then fed into a compute shader that generates the geometry for a single blade. The number of blade segments can be customized. To add a realistic feeling to the grass, the following transformations are also applied to each blade: a random jitter to the anchor point because of the grid-like pattern of the sampling algorithm; a random rotation that sets which direction the blade is oriented; a random bend for the tip of the blade and a random scaling. After these transformations, the points are returned to world space coordinates to be placed over the terrain. Finally, a shader applies a grass texture to each leaf to add volume and color.

Approximately 4 million blades of grass, each composed of 9 points, can be generated and updated at 20 ~ 30 fps in the mentioned hardware, displaying all grass blades simultaneously. It is worth noting that this instancing method is not used with trees, bushes, and other plants because the random jitter prevents us from enforcing a minimum radius distance between instanced objects to avoid collisions.

**Repeatability** Each scene is generated by a seed to ensure repeatability. This seed is transmitted to every vegetation pipeline and to the grass and terrain generators. Fig. 2 shows an example of the pipelines for generating trees and grass and a top-down view of the resulting forest scene, and Fig. 3 shows the same scene from a front view and a closer view.

**Point Cloud Extraction** The point cloud of the generated scene can be extracted directly from the Unity Editor as a .csv file. By tagging the instanced objects with meshes, they can be exported as various categories, including but not limited to terrain, canopy, trunk, branches, bushes, understory, grass, cacti, and deadwood, assigning the corresponding label to each point of the point cloud. The size of the scene’s point cloud can be altered by adding more points to the

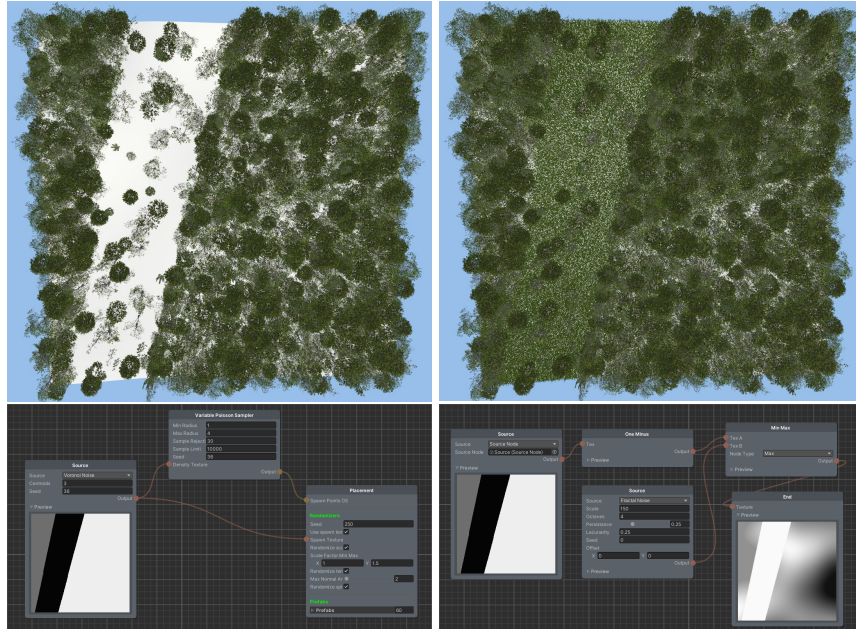


Fig. 2: Above: Forest scene with trees (left), and trees, bushes, and grass (right). Below: the correspondence pipelines for instancing trees (left), and grass (right).

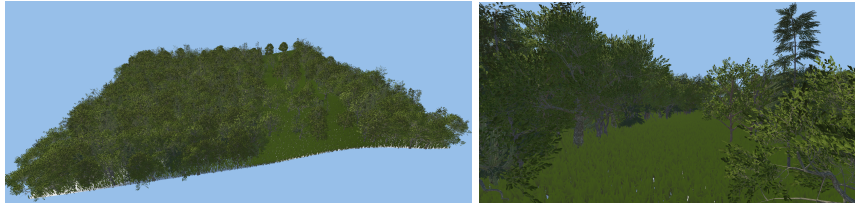


Fig. 3: Left: Frontal view of a generated forest scene. Right: Close up view.

terrain mesh, by generating more grass leaves or changing their number of segments, or by importing other vegetation prefabs with the desired quantity. This customization helps generating scenes where its point cloud can vary in size, and thus be adapted to specific needs, such as training large deep learning networks.

As one of the contributions of this work, the code of the presented forest simulator was released at <https://github.com/lrse/forest-simulator>.

### 3.3 Dataset Assembling

Two datasets were created to train the selected deep learning architectures, simulating the point clouds obtained by LiDAR and applying structure from motion algorithm to synthetic camera images, both from a top-down view. For

the camera-like dataset, a method to include occlusion to the point cloud was used [46], as several points should not be visible from a top-down view of the forest. Then, random noise with zero mean is added to give variability to the point clouds, and it is partitioned in the  $xy$  plane using  $K$ -Means clustering to assemble subclouds with which to train the networks. Both datasets, LiDAR-like and Camera-like, are publicly at <https://github.com/lrse/synthetic-forest-datasets> to ensure this work’s results are reproducible and to increase the point cloud datasets available to the scientific community.

The Evo Dataset, given by [12], was employed to test the trained architectures. We used an occluded version of this dataset to test the architectures trained with the Camera-like dataset, using the same occlusion method [46].

To create a synthetic dataset that resembles the Evo Dataset, we have extracted four categories from the simulator: terrain, trunks, canopy, and understory, the latter including grass, bushes, and all other vegetation that are not trees. In Fig. 4, an example of both datasets segmented using  $K$ -means and segmented into the studied categories can be seen.

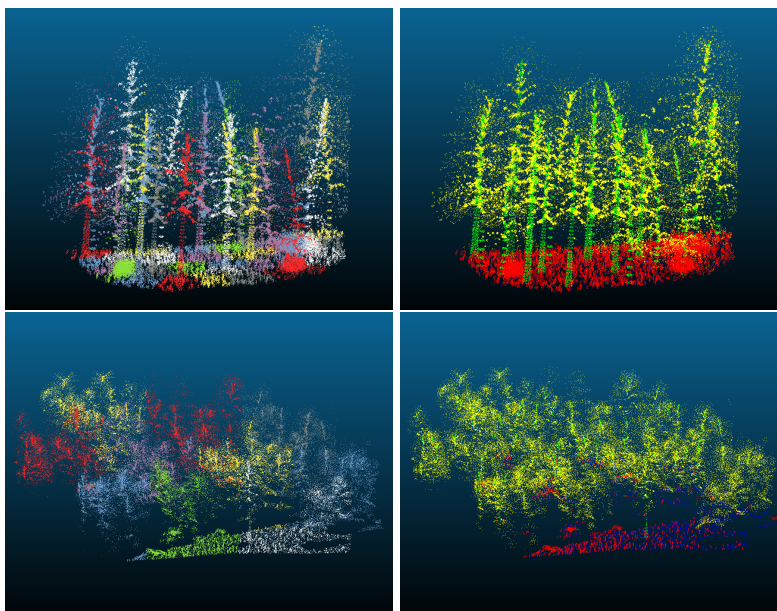


Fig. 4: Above: Example scene without occlusion segmented using  $K$ -Means (left) and segmented via labels: blue, green, yellow, and red corresponding to terrain, trunks, canopy, and understory, respectively (right). Below: Same example for another scene, but using occlusion from a top-view point.

## 4 Results and Discussion

For experimental results, the four selected architectures were trained with an AMD Phenom II X6 1075T Processor CPU, with 32GB RAM, and two NVIDIA RTX 3090 connected with an SLI bridge. 50 epochs were used for every network, with an average training time of 472 seconds per epoch for the LiDAR-like dataset and 239 seconds for the Camera-like dataset.

### 4.1 LiDAR-like experiment

Table 1 shows the results of testing the networks trained with the LiDAR-like dataset with the Evo dataset. The confusion matrix of each network is presented in Table 2. It can be seen that, regardless of having an overall good accuracy, the networks still struggle to differentiate understorey from terrain, especially when the vegetation is on a near-ground level. Despite this, in Section 4.3 we show that the networks perform well in segmenting the trees from the rest of the categories. PointNeXt had a better result in classifying the points in the Evo dataset and segmenting each category, and therefore it seems more suitable for LiDAR datasets.

Table 1: Results obtained testing both on the created Synthetic Forest Dataset and in the Evo dataset, using the LiDAR-like dataset.

Network	Synthetic Forest Dataset			Evo Dataset		
	Overall Accuracy	Class Avg. Accuracy	Class Avg. mIoU	Overall Accuracy	Class Avg. Accuracy	Class Avg. mIoU
PointNeXt	0.9348	0.8339	0.7314	<b>0.7695</b>	0.6436	<b>0.5153</b>
PointBERT	0.9551	0.8719	0.8021	0.7195	<b>0.6462</b>	0.4206
PointMAE	<b>0.9575</b>	<b>0.8743</b>	<b>0.8029</b>	0.72788	0.61103	0.4278
PointGPT	0.9414	0.8257	0.7516	0.6417	0.5271	0.3620

Table 2: Confusion matrix for the four studied networks.

PointNeXt					PointBERT				
	Terrain	Trunk	Canopy	Understorey		Terrain	Trunk	Canopy	Understorey
Terrain	<b>1055469</b>	4234	423	386498	Terrain	756515	16905	6451	<b>1314363</b>
Trunk	468	<b>191869</b>	135275	59160	Trunk	3386	<b>401490</b>	184272	67868
Canopy	10201	254302	<b>8310787</b>	1220544	Canopy	11031	1088940	<b>6703359</b>	765463
Understorey	1105198	21323	1067	<b>1128622</b>	Understorey	373703	38963	22493	<b>2129238</b>

PointMAE					PointGPT				
	Terrain	Trunk	Canopy	Understorey		Terrain	Trunk	Canopy	Understorey
Terrain	315040	2506	18805	<b>1756467</b>	Terrain	363932	8427	13425	<b>1709711</b>
Trunk	193	<b>340098</b>	187716	129111	Trunk	593	219103	206613	<b>229875</b>
Canopy	6316	779671	<b>6986603</b>	796919	Canopy	11898	1049754	<b>5682647</b>	1824946
Understorey	49187	13302	38252	<b>2465254</b>	Understorey	112227	23866	31023	<b>2387380</b>

## 4.2 Camera-like experiment

Table 3 shows the results of testing the networks trained with the Camera-like dataset with the Evo dataset with occlusion. The confusion matrices of each network can be seen in Table 4. Similar to the previous case, the networks struggle to differentiate terrain points from understory points, and as few trunk points remain visible, especially the ones at the base of the trunk, it is also often confused with understory points. We can see that the overall performance is significantly lower than in the case without occlusion. Again, when considering only two categories, Tree and Non-tree, the overall accuracy achieves better results (see Section 4.3). PointMAE obtains slightly better accuracy than the other networks, although all have similar responses.

Table 3: Results obtained testing both on the created Synthetic Forest Dataset and in the Evo dataset, using the Camera-like dataset.

Network	Synthetic Forest Dataset			Evo Dataset		
	Overall Accuracy	Class Avg. Accuracy	Class Avg. mIoU	Overall Accuracy	Class Avg. Accuracy	Class Avg. mIoU
PointNeXt	<b>0.9497</b>	0.6875	0.5926	0.6236	0.4868	0.4120
PointBERT	0.9369	0.7246	0.6303	0.6549	0.5085	<b>0.4533</b>
PointMAE	0.9401	<b>0.7289</b>	<b>0.6419</b>	<b>0.6822</b>	<b>0.5448</b>	0.4248
PointGPT	0.9336	0.7180	0.6175	0.5794	0.5445	0.3909

Table 4: Confusion matrix for the four studied networks.

PointNeXt					PointBERT				
	Terrain	Trunk	Canopy	Understorey		Terrain	Trunk	Canopy	Understorey
Terrain	<b>6566</b>	0	0	6229	Terrain	<b>8923</b>	0	0	5388
Trunk	68	0	24	<b>299</b>	Trunk	102	23	40	<b>484</b>
Canopy	100	0	<b>6990</b>	909	Canopy	140	2	<b>6226</b>	639
Understorey	2391	0	0	<b>3048</b>	Understorey	<b>2392</b>	0	0	2265

PointMAE					PointGPT				
	Terrain	Trunk	Canopy	Understorey		Terrain	Trunk	Canopy	Understorey
Terrain	<b>9508</b>	0	0	4653	Terrain	<b>7283</b>	3	0	7069
Trunk	71	75	38	<b>445</b>	Trunk	80	219	25	<b>308</b>
Canopy	108	18	<b>6028</b>	951	Canopy	137	415	<b>5278</b>	1126
Understorey	2176	0	0	<b>2553</b>	Understorey	2018	17	0	<b>2646</b>

## 4.3 Tree and Non-Tree segmentation

Table 5 shows the results obtained considering only Tree and Non-Tree categories, the first one including trunk and canopy points, and the latter including terrain and understory points, training with both datasets, LiDAR-like and

Table 5: Results obtained considering the categories Tree and Non-Tree, testing in the Evo dataset and training in both the LiDAR-like and the Camera-like datasets.

Network	LiDAR-like Dataset			Camera-like Dataset		
	Overall Accuracy	Class Avg. Accuracy	Class Avg. mIoU	Overall Accuracy	Class Avg. Accuracy	Class Avg. mIoU
PointNeXt	0.9051	0.9330	0.8035	0.9414	<b>0.9180</b>	0.8765
PointBERT	<b>0.9328</b>	<b>0.9449</b>	<b>0.8652</b>	<b>0.9487</b>	0.9108	<b>0.8773</b>
PointMAE	0.9276	0.9416	0.8561	0.9408	0.8982	0.8596
PointGPT	0.8454	0.8797	0.7252	0.9372	0.8906	0.8497

Camera-like, and testing with the Evo Dataset. It can be seen that the tree segmentation obtains a high accuracy percentage with all the considered networks, being PointBERT the one with better results.

## 5 Conclusions and future work

In this work, we developed an open-source simulator based on Unity Engine that generates realistic forest scenes procedurally. With it, we have created synthetic point-based datasets, with each point labeled into one of the categories: terrain, trunk, canopy, and understory (including grass, bushes, and other vegetation that are not trees). We then employed these datasets to train four state-of-the-art deep-learning point-based networks. Finally, we tested and compared them in the real forest Evo dataset. The results show that synthetic point cloud data can be used to train deep-learning networks for posterior forest segmentation with real data. Among the tested networks, PointNeXt seemed to give better results when trained with the LiDAR-like dataset than the other networks, whereas PointMAE obtained slightly better accuracy when trained with the Camera-Like dataset. When considering only two categories, Tree and Non-tree, a higher accuracy percentage is obtained, and PointBERT achieved better results than the other networks.

As future work, we will use synthetic data to pre-train the deep learning networks and then fine-tune them using real data, expecting better accuracy, specially in the experiments that considers the four categories (terrain, trunks, canopy and understory). This result is also relevant since it would allow data collection in only a portion of the forest area of interest to conduct deep learning network training.

## References

1. Murtiyoso, A., Holm, S., Riihimäki, H., Krucher, A., Griess, H., Griess, V. C., Schweier, J: Virtual forests: a review on emerging questions in the use and application of 3D data in forestry. *International Journal of Forest Engineering* **35**(1), 29–42 (2024)

2. Guimarães, N., Pádua, L., Marques, P., Silva, N., Peres, E., Sousa, J. J.: Forestry remote sensing from unmanned aerial vehicles: A review focusing on the data, processing and potentialities. *Remote Sensing* **12**(6), 1046 (2020)
3. Pessacq, F., Gómez-Fernández, F., Nitsche, M., Chamo, N., Torrella, S., Ginzburg, R., De Cristóforis, P.: Simplifying UAV-based photogrammetry in forestry: How to generate accurate digital terrain model and assess flight mission settings. *Forests* **13**(2), 173 (2022)
4. Guo, Y., Wang, H., Hu, Q., Liu, H., Liu, L., Bennamoun, M.: Deep learning for 3d point clouds: A survey. *IEEE transactions on pattern analysis and machine intelligence* **43**(12), 4338–4364 (2020)
5. Dai, A., Chang, A. X., Savva, M., Halber, M., Funkhouser, T., Nießner, M.: Scannet: Richly-annotated 3d reconstructions of indoor scenes. In: *Proceedings of the IEEE conference on computer vision and pattern recognition*, pp. 5828–5839. IEEE Xplore, Honolulu, United States of America (2017)
6. Uy, M. A., Pham, Q. H., Hua, B. S., Nguyen, T., Yeung, S. K.: Revisiting point cloud classification: A new benchmark dataset and classification model on real-world data. In: *Proceedings of the IEEE/CVF international conference on computer vision*, pp. 1588–1597. IEEE Xplore, Seoul, Korea (2019)
7. Wu, Z., Song, S., Khosla, A., Yu, F., Zhang, L., Tang, X., Xiao, J.: 3d shapenets: A deep representation for volumetric shapes. In: *Proceedings of the IEEE conference on computer vision and pattern recognition*, pp. 1912–1920. IEEE Xplore, Boston, United States of America (2015)
8. Yi, L., Kim, V. G., Ceylan, D., Shen, I. C., Yan, M., Su, H., Lu, C., Huang, Q., Sheffer, A., Guibas, L.: A scalable active framework for region annotation in 3d shape collections. *ACM Transactions on Graphics* **35**(6), 1–12 (2016)
9. Behley, J., Garbade, M., Milioto, A., Quenzel, J., Behnke, S., Stachniss, C., Gall, J.: Semantickitti: A dataset for semantic scene understanding of lidar sequences. In: *Proceedings of the IEEE/CVF international conference on computer vision*, pp. 9297–9307. IEEE Xplore, Seoul, Korea (2019)
10. Jin, S., Su, Y., Zhao, X., Hu, T., Guo, Q.: A point-based fully convolutional neural network for airborne lidar ground point filtering in forested environments. *IEEE journal of selected topics in applied earth observations and remote sensing* **13**, 3958–3974 (2020)
11. Krisanski, S., Taskhiri, M. S., Gonzalez Aracil, S., Herries, D., Turner, P.: Sensor agnostic semantic segmentation of structurally diverse and complex forest point clouds using deep learning. *Remote Sensing* **13**(8), 1413 (2021)
12. Kaijaluoto, R., Kukko, A., El Issaoui, A., Hyypä, J., Kaartinen, H.: Semantic segmentation of point cloud data using raw laser scanner measurements and deep neural networks. *ISPRS Open Journal of Photogrammetry and Remote Sensing* **3**, 100011 (2022)
13. Unity Homepage, <https://unity.com/>. Last accessed 20 Feb 2024
14. Gevaert, C. M., Persello, C., Nex, F., Vosselman, G.: A deep learning approach to DTM extraction from imagery using rule-based training labels. *ISPRS journal of photogrammetry and remote sensing* **142**, 106–123 (2018)
15. Amirkolaei, H. A., Arefi, H., Ahmadlou, M., Raikwar, V.: DTM extraction from DSM using a multi-scale DTM fusion strategy based on deep learning. *Remote Sensing of Environment* **274**, 113014 (2022)
16. Li, S., Xiong, L., Tang, G., Strobl, J.: Deep learning-based approach for landform classification from integrated data sources of digital elevation model and imagery. *Geomorphology* **354**, 107045 (2020)

17. Hu, X., Yuan, Y.: Deep-learning-based classification for DTM extraction from ALS point cloud. *Remote sensing* **8**(9), 730 (2016)
18. Lê, H. Â., Guiotte, F., Pham, M. T., Lefèvre, S., Corpetti, T.: Learning Digital Terrain Models From Point Clouds: ALS2DTM Dataset and Rasterization-Based GAN. *IEEE Journal of Selected Topics in Applied Earth Observations and Remote Sensing* **15**, 4980–4989 (2022)
19. Li, B., Lu, H., Wang, H., Qi, J., Yang, G., Pang, Y., Dong, H., Lian, Y.: Terrain-Net: A Highly-Efficient, Parameter-Free, and Easy-to-Use Deep Neural Network for Ground Filtering of UAV LiDAR Data in Forested Environments. *Remote Sensing* **14**(22), 5798 (2022)
20. Qi, C. R., Yi, L., Su, H., Guibas, L. J.: Pointnet++: Deep hierarchical feature learning on point sets in a metric space. *Advances in neural information processing systems* **30** (2017)
21. Ronneberger, O., Fischer, P., Brox, T.: U-net: Convolutional networks for biomedical image segmentation. In: *Medical Image Computing and Computer-Assisted Intervention–MICCAI 2015: 18th International Conference. Proceedings, Part III 18*, pp. 234–241. Springer International Publishing, Munich, Germany (2015)
22. Thomas, H., Qi, C. R., Deschaud, J. E., Marcotegui, B., Goulette, F., Guibas, L. J.: Kpconv: Flexible and deformable convolution for point clouds. In: *Proceedings of the IEEE/CVF international conference on computer vision*, pp. 6411–6420. IEEE Xplore. Seoul, Korea (2019)
23. Wu, W., Qi, Z., Fuxin, L.: Pointconv: Deep convolutional networks on 3d point clouds.. In: *Proceedings of the IEEE/CVF Conference on computer vision and pattern recognition*, pp. 9621–9630. IEEE Xplore. California, United States of America (2019)
24. Boulch, A.: ConvPoint: Continuous convolutions for point cloud processing. *Computers & Graphics* **88**, 24–34 (2020)
25. Lu, J., Liu, T., Luo, M., Cheng, H., Zhang, K.: PFCN: a fully convolutional network for point cloud semantic segmentation. *Electronics Letters* **55**(20), 1088–1090 (2019)
26. Qian, G., Li, Y., Peng, H., Mai, J., Hammoud, H., Elhoseiny, M., Ghanem, B.: Pointnext: Revisiting pointnet++ with improved training and scaling strategies. *Advances in Neural Information Processing Systems* **35**, 23192–23204 (2022)
27. Vaswani, A., Shazeer, N., Parmar, N., Uszkoreit, J., Jones, L., Gomez, A. N., Kaiser, L., Polosukhin, I.: Attention is all you need. *Advances in neural information processing systems* **30** (2017)
28. Engel, N., Belagiannis, V., Dietmayer, K.: Point transformer. *IEEE access* **9**, 134826–134840 (2021)
29. Zhao, H., Jiang, L., Jia, J., Torr, P. H., Koltun, V.: Point transformer. In: *Proceedings of the IEEE/CVF international conference on computer vision*, pp. 16259–16268. IEEE Xplore, Virtual (2021)
30. Park, C., Jeong, Y., Cho, M., Park, J.: Fast point transformer. In: *Proceedings of the IEEE/CVF Conference on Computer Vision and Pattern Recognition*, pp. 16949–16958. IEEE Xplore, New Orleans, United States of America (2022)
31. Guo, M. H., Cai, J. X., Liu, Z. N., Mu, T. J., Martin, R. R., Hu, S. M.: Pct: Point cloud transformer. *Computational Visual Media* **7**, 187–199 (2021)
32. Yu, X., Tang, L., Rao, Y., Huang, T., Zhou, J., Lu, J.: Point-bert: Pre-training 3d point cloud transformers with masked point modeling. In: *Proceedings of the IEEE/CVF Conference on Computer Vision and Pattern Recognition*, pp. 19313–19322. IEEE Xplore, New Orleans, United States of America (2022)

33. Devlin, J., Chang, M. W., Lee, K., Toutanova, K. N.: BERT: Pre-training of Deep Bidirectional Transformers for Language Understanding. arXiv preprint arXiv:1810.04805 (2016)
34. Bao, H., Dong, L., Piao, S., Wei, F.: BEiT: BERT Pre-Training of Image Transformers. In: International Conference on Learning Representations (2022)
35. Rolfe, J. T.: Discrete Variational Autoencoders. In: 9th International Conference on Learning Representations (2017)
36. Pang, Y., Wang, W., Tay, F. E., Liu, W., Tian, Y., Yuan, L.: Masked autoencoders for point cloud self-supervised learning. In: EComputer Vision–ECCV, pp. 604–621. Springer (2022)
37. He, K., Chen, X., Xie, S., Li, Y., Dollár, P., Girshick, R.: Masked autoencoders are scalable vision learners. In: Proceedings of the IEEE/CVF conference on computer vision and pattern recognition, pp. 16000–16009. IEEE Xplore, New Orleans, United States of America (2022)
38. Chen, G., Wang, M., Yang, Y., Yu, K., Yuan, L., Yue, Y.: PointGPT: Auto-regressively Generative Pre-training from Point Clouds. *Advances in Neural Information Processing Systems* **36** (2024)
39. Radford, A., Narasimhan, K., Salimans, T., Sutskever, I.: Improving language understanding by generative pre-training. In preprint (2018)
40. Morton, G. M.: A computer oriented geodetic data base and a new technique in file sequencing. International Business Machines Company New York (1966)
41. Nunes, R., Ferreira, J. F., Peixoto, P.: Procedural generation of synthetic forest environments to train machine learning algorithms. In: ICRA 2022 Workshop in Innovation in Forestry Robotics: Research and Industry Adoption (2022)
42. SynPhoRest Dataset Homepage, <https://zenodo.org/records/6369446>. Last accessed 21 Feb 2024
43. Russell, D. J., Arevalo-Ramirez, T., Garg, C., Kuang, W., Yandun, F., Wettergreen, D., Kantor, G.: UAV Mapping with Semantic and Traversability Metrics for Forest Fire Mitigation. In: ICRA 2022 Workshop in Innovation in Forestry Robotics: Research and Industry Adoption (2022)
44. Bridson, R.: Fast Poisson disk sampling in arbitrary dimensions. *SIGGRAPH sketches* **10**(1), 1 (2007)
45. TreeIt Homepage, <http://www.evolved-software.com/treeit/treeit>. Last accessed 27 Feb 2024
46. Katz, S., Tal, A., Basri, R.: Direct visibility of point sets. *ACM Transactions on Graphics* **26**(3), 24 (2007)